SAND2017-11256J

Non-Destructive Evaluation of the Bondline Interface between Carbon Fiber Reinforced Laminated Composites and Metal Materials via Ultrasonic Inspection Methods

Sarah L. Stair[1], David G. Moore[2], David A. Jack[1] and Ciji L. Nelson[2]

[1]Department of Mechanical Engineering
Baylor University, Waco, Texas, 76798
[2]Nondestructive Evaluation and Experimental Mechanics Department
Sandia National Laboratories, Albuquerque, New Mexico, 87185

Abstract: Woven fiber, laminated composites allow the design engineer to create high strength parts, but the effectiveness of the final processed part is greatly diminished through weak or nonexistent bonds between the composite and the substrate to which it is bonded. These layered laminates are commonly made by curing the resin infused carbon fiber fabrics in predefined layers and then bonding them to another composite or a metallic structure using either a pre-cure or a co-cure method. The focus of this study is the identification of the defect caused by a disbond or a delamination located at the interface between a composite laminate stack and the substrate to which it is bonded. We present a nondestructive approach using various ultrasonic methods to identify the existence of the bond between composite and composite-to-metal interface. This paper explores contact and immersion ultrasound methods using pulse-echo for evaluating the composite material and adhesive bondline and the signal attenuation undergone by the wave as it propagates through the composite. Finally, a summary of the detection and analysis techniques developed to identify disbonds, including Fast Fourier Transform analysis of the immersion data, is presented. Each of the methods evaluated in this study is able to detect the transition from bonded to unbonded sections at the bondline from either side of the bonded part, with the immersion technique providing a significantly higher resolution of the edge of the bondline.

1.0 – Introduction

Carbon fiber reinforced laminated composites are used in a wide variety of industries, such as automotive and aerospace, both as prime structures and as part of their repair processes. Their selection as a material is often made due to their high strength to weight ratio. A common manufacturing technique to expand the application space of composites involves joining a composite structure with a second structure through the use of an adhesive bond. This paper seeks to quantify the presence of this adhesive bond in a nondestructive manner.

Unlike many metallic structures, fiber reinforced laminated composites are nonhomogeneous materials that often have multiple degrees of anisotropy with respect to material properties. Within the composite there are often a variety of defects including: voids (porosity), delaminations, matrix cracking, and poor bonding between the fiber and the resin matrix to name a few [1, 2]. Each of these defects affects the mechanical behavior and quality of the final, as-manufactured laminate. Vine, *et al.* [3] evaluated a variety of environmental effects on the adhesive bond between two materials. Nieminen and Koenig [4] stated that the condition of an adhesive joint could be characterized with a destructive technique, such as peel and tensile tests. However, with increased applications involving the joining of composite and metal structures, a

nondestructive evaluation method for inspecting the quality of the bondline between these two dissimilar materials is desired.

Studies performed by Ting [5] and Ting and Sachse [6] examined how the viscoelastic nature of the resin binding the carbon fibers will disperse and weaken the ultrasound wave as it propagates through the sample thickness. The classical Snell's Law discusses how at a material interface a portion of the incident wave will reflect back toward the pulser (sound source) while the remainder of the wave refracts into the next material. Nikitin *et al.* [7] observed this behavior within a multi-layered laminated composite and were able to detect many reflection/refraction pairs as compared to a homogeneous material, such as aluminum.

Baker [8, 9] provides an excellent overview of acceptable methods in the international aerospace industry for the inspection and repair process of bonded aluminum components. Baker contrasted the bond repair using a composite patch with that of using a mechanical repair with fasteners, and in one of the studies the development of an in-situ method called the "Smart Patch approach", which incorporates embedded strain gages and sensors, for structural health monitoring within the patch repair was proposed.

Nieminen and Koenig [4] provide a description of macroscopic and microscopic NDE methods for evaluating the bond between two aluminum structures, structures with honeycomb materials and composite structures. Their methods include coin tapping, mechanical impedance technique, radiography, and thermography, but they emphasized the use of ultrasound methods for inspecting the bond between these materials. Adams and Cawley [10] also describe the different types of bondline defects, such as zero volume voids, disbonds, and the presence of release agents which chemically weaken the bond, that can occur between adherends and discuss NDE methods for identifying them, such as ultrasound, eddy current testing, passive and active thermographic approaches, and optical holography. Wang, *et al.* [11] monitored the ultrasound signal at various stages of an adhesive's cure cycle and noted that the reflection coefficient, the amount of the wave that is reflected at a material interface, varied throughout the curing process.

The early work related to ultrasound inspection of bondline interfaces was performed on aluminum-aluminum bonded samples due to their relevance in the aerospace industry. Cawley and Hodson [12] used an ultrasonic spectroscopy method to inspect the bondline between two aluminum plates with accuracy similar to that of destructive sectioning techniques. Drinkwater and Cawley [13] ultrasonically inspected the bondline between two clamped aluminum plates in contact but with no adhesive. By varying the applied pressure on the plates, Drinkwater and Cawley observed a frequency dependence of the reflection coefficient. In general, as the pressure increased and the plates were in closer contact with one another, the reflection coefficient decreased, which is to be expected. Drinkwater, *et al.* [14] studied the relationship between repeated loading cycles and the measured reflection coefficient at the bondline between the aluminum plates. They noted that after the first loading cycle, which included some plastic deformation on the contacting surfaces of the two plates, the cyclic loading and measured reflection coefficient were repeatable. Vine, *et al.* [15] inspected the bondline between aluminum plates using an ultrasound technique that combined normal and oblique incidence waves. To degrade the bondline, the samples were exposed to a water bath at an elevated temperature for varying amounts of time. The selected adhesive was sensitive to water, and when it came in

contact with water, the adhesive began to plasticize and degrade. Using the combination of oblique and normal incidence ultrasound waves, Vine, *et al.* were able to detect weak regions of the bond between the aluminum plates. Pilarski and Rose [16] performed a similar experiment, but instead of looking at aluminum plates bonded to one another, their study focused on the bond between aluminum and a layer of epoxy. Their experiment applied a through transmission, oblique incidence angle ultrasound approach for inspecting the bondline between the aluminum and epoxy. Pilarski and Rose [16] stated that the oblique incidence provided a higher difference in signal amplitude between the poorly bonded and well-bonded areas. Although their study is similar to the one presented in this paper in that it evaluated the bondline between two dissimilar materials, the present study focuses on the inspection of a bondline between aluminum and a carbon fiber reinforced laminated composite, which has a higher degree of anisotropy compared to neat epoxy. Due to the complexity of the laminate structure, a normal incidence approach was used for the present study, and because this technique is being developed while keeping repair processes in mind, a pulse-echo technique was applied in the present study because a technician may only have access to one side of the part during the inspection.

Drinkwater, *et al.* [17] extended their previous work in [13] and evaluated the relationship between applied pressure and the measured reflection coefficient of two graphite bricks in contact with one another. Using the measured reflection coefficient, Drinkwater, *et al.* [17] estimated the stiffness at the interface and compared their results with those obtained using the contact model developed by Webster and Sayles [18]. There was a discrepancy between the model and their measurements, but the discrepancy was attributed to the estimated modulus of the graphite sample.

Vijaya Kumar, *et al.* [19] used a combination of normal and oblique incident ultrasound waves to inspect the bondline between two unidirectional laminated composites. To induce varying amounts of degradation into the bondline between the two laminates, they added polyvinyl alcohol, a mold release agent, into the epoxy adhesive. As the epoxy adhesive cured, the polyvinyl alcohol induced porosity between the two laminates. Vijaya Kumar, *et al.* [19] found that increased porosity led to increased degradation at the bondline and an increased reflection coefficient. The present authors in [20] considered the ultrasonic inspection of carbon fiber reinforced laminated composites bonded to an aluminum plate and found that the contact transducer technique, the immersion ultrasound technique and the phased array ultrasound technique used in the study were all able to identify unbonded and bonded areas between the composite and aluminum.

The sources described thus far have outlined the research that has been performed regarding nondestructive, ultrasound methods for analyzing the bondline between two materials. The studies have considered the pressure applied to the adherends, normal versus oblique incident angles used during inspection, and how the degree of cure affects the bondline inspection results. The present study expands upon the initial work in [20] by further analyzing the contact transducer and immersion technique results (see e.g., [21]) including a more detailed discussion of the results obtained for various composite thicknesses as well as evaluating the frequency content associated with bonded and unbonded locations at the interface between the aluminum and the carbon fiber reinforced laminated composite.

2.0 – Sample Fabrication

Aluminum 6061 sheet stock 6.35 mm in thickness was cut into a rectangular section of 101.6 mm by 304.8 mm. The thickness was then milled down to thicknesses of 5.41 and 4.57 mm as depicted in Figure 1. The steps were designed to accommodate composite laminates of: 4, 8, and 12 lamina, respectively, while maintaining a relatively "flat" inspection surface. An 8 harness-satin weave preimpregenated with UF3352 Resin was used for each sample. The 8 harness-satin weave is sensitive to orientation and structurally is not periodic every 90 degrees, but rather every 180 degrees. Thus a 0 degree and a 90 degree orientation will yield different structural behavior. The ply stacks were constructed to be symmetric and balanced, with the ply stacks for the 4, 8 and 12 ply stacks given, respectively, as $[0/90]_{2,s}$, $[0/90]_{4,s}$ and $[0/90]_{6,s}$. The notation $[0/90]_{2n,s}$ implies there are a total of 2n lamina in a symmetric pattern, with the ply orientation being defined as away from the centerline. For example, the $[0/90]_{4,s}$ says the outer lamina are each 0 degrees, followed by a 90, then a 0, then a 90 for a total ply stack of [0,90,0,90,90,0,90,0]. Notice in Figure 1 that the "End view" shows a cross-sectional view of the sample taken with an optical microscope of the 12 ply laminate. The aluminum material is artificially drawn into the image and is depicted by the solid colored area at the bottom of the image. The optical image highlights the center plane of the 12 ply laminate, where the axis of symmetry in the laminate stacking sequence is observed.

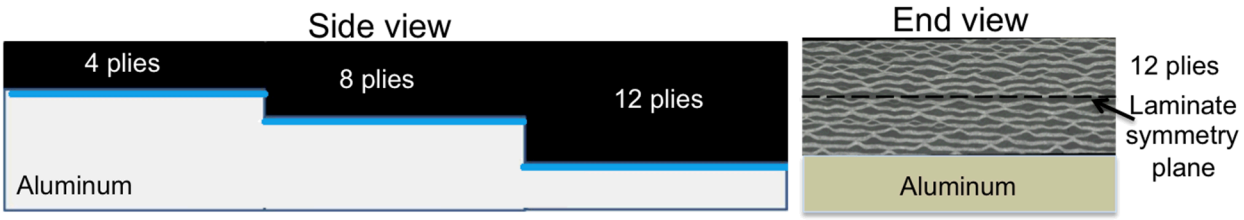

Fig. 1. Specimens are constructed of carbon fiber reinforced plastic (CFRP) $[4 \text{ ply } [0/90]_2]_s$ $8 \text{ ply } [0/90]_4]_s$ and $12 \text{ ply } [0/90]_6]_s$ preimpregnated 8 harness-satin weave with UF3352 TCR™ Resin

Two different fabrication methods for the bonding of the above samples are presented in this study. The first sample fabricated is an eight-harness satin weave carbon fiber laminate preimpregnated with UF3352 TCR^{TM} resin, and a release agent was placed on the aluminum wedge plate depicted in Figure 1 to prevent the sample from curing to the aluminum. After cure the part was free from the aluminum tooling and a coupling material, in this case the Soundsafe gel couplant made by Sonotech, was placed at the bondline between the two materials for later imaging. This method of manufacturing the sample is called a pre-cure method. The second sample was manufactured using a co-curing technique to bond the aluminum with the carbon fiber laminate. This second sample was manufactured using the eight-harness satin weave carbon fiber fabric that was preimpregnated with UF3352 TCR^{TM} resin placed onto the step wedge aluminum plate prior to the laminate's cure cycle. As the laminate underwent its cure cycle, the two materials were bonded to one another as the resin matrix formed crosslinks and solidified. Both of the investigated manufacturing techniques, the pre-cure and co-cure techniques, have been used in the aerospace industry while making composite repairs to aluminum aircraft [8, 9], and in this study we seek to identify potential differences in the bond quality produced by these two methods.

3.0 – Bondline Detection with Contact Transducer Ultrasonics

The bondline between the pre-cured carbon fiber reinforced laminated composite and the step wedge aluminum plate is first inspected using a 5 MHz contact ultrasound transducer. The contact transducer method is a commonly used ultrasound method for inspecting parts and identifying defects [5] and has a planar resolution similar to that of the probe diameter. This technique is performed in the present study for two reasons: first, to determine whether or not the method is able to identify the difference between bonded and unbonded regions at the composite-to-metal interface, and second, to have a baseline by which to compare the high resolution immersion ultrasound results presented in the following section.

To simulate an unbonded structure, no acoustic couplant is placed between the laminated composite and the aluminum. For the bonded case, a Soundsafe couplant made by Sonotech is used to acoustically couple the two materials to one another. This gel couplant simulates an adhesive bond between the two materials.

Figure 2(a) shows the setup used in the contact transducer inspection when the inspector has access to only the aluminum side. The transducer is placed in contact with the aluminum surface with a thin layer of an acoustic gel couplant placed between the transducer and the aluminum. The ultrasound wave propagates through the aluminum to the metal-to-composite bondline and then into the composite. Figures 2(b) and 2(c) each contain an A-scan amplitude plot (top images) and a Fast Fourier Transform plot of the gated region indicated in the A-scans (lower images). Figure 2(b) corresponds to an unbonded case where no acoustic couplant was placed between the carbon fiber reinforced laminated composite and the aluminum for the 12 ply laminate region of Figure 1, but the results presented yield the same conclusions for all thicknesses. Figure 2(c) corresponds to the case where a layer of couplant is present between the two materials, thus providing an acoustic path for the ultrasound wave propagation.

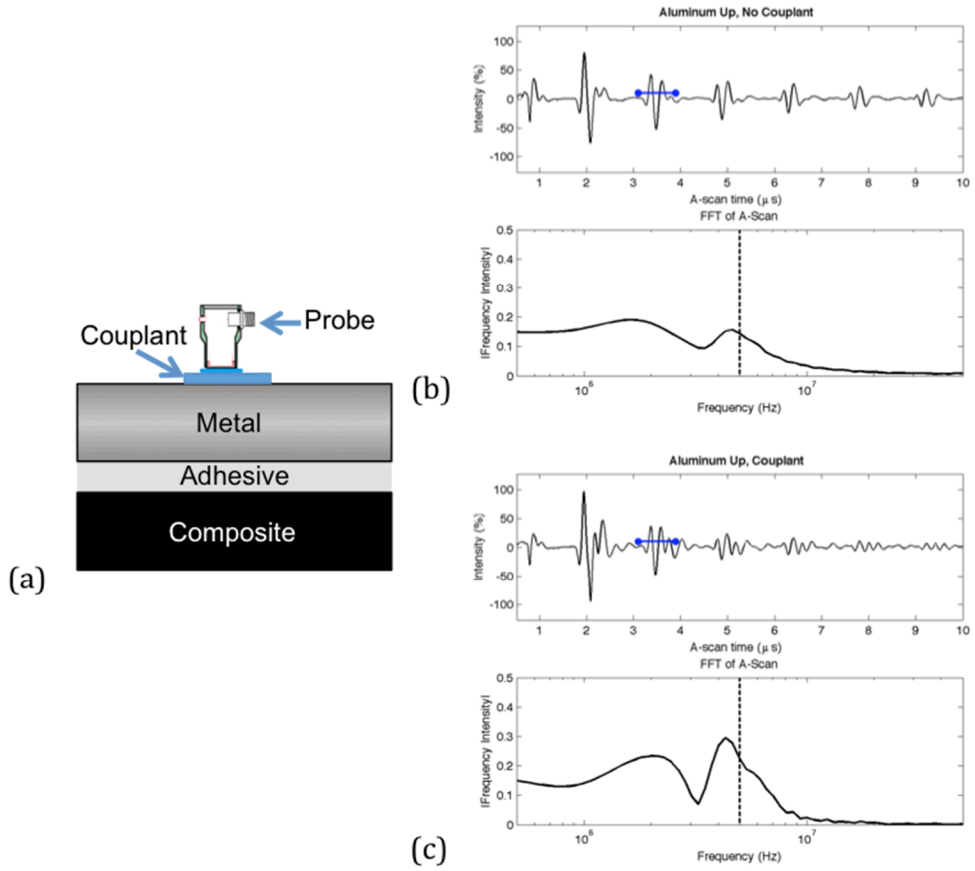

Fig. 2: Inspection of the sample using a 5 MHz contact transducer. (a) The experimental configuration of the contact transducer measurements with the metal in contact with the transducer. The A-scan results (top image) and Fast Fourier Transform results (lower image) for, respectively, (b) an *unbonded* and (c) a *bonded* section of the interface. The dashed line in (b) and (c) refers to the peak transducer frequency.

In Figure 2, the difference in the shape of A-scan obtained for the unbonded case versus that obtained for the bonded case is evident by a comparison of the amplitude associated with the ringing within the aluminum section of the part. The intensity of the ringing is observed to decrease more quickly for the bonded component, whereas the ringing continues for a longer period of time and with higher signal amplitude for the unbonded part. This is most evident within the gate marked by the blue horizontal line in the A-scan in Figures 2(b) and 2(c), where the signal intensity for the bonded part is observed to decay noticeably. Upon further ringing the intensity of the signal for the bonded case continues to drop precipitously. This observed difference in amplitude is explained by the reflection coefficient for the different material interfaces as well as the signal attenuation that occurs within the composite. As the ultrasound wave encounters the unbonded interface, the wave is approaching an aluminum to air boundary. The acoustic impedance for air, the medium within the gap, is near zero meaning that the majority of the wave is reflected back through the aluminum and returns to the contact transducer from which the signal originated. When the wave encounters a bonded interface, it approaches a metal-to-composite boundary, and a portion of the ultrasound wave propagates into the composite laminate with the remainder reflecting back into the aluminum. This loss in signal energy contributes to a decrease in the signal amplitude as well as an expansion of the signal duration observed from the return signal and is observed in Figure 2(c). However, it is important

to note that regardless of the type of material bonded to the aluminum, the signal amplitude will always exhibit some amplitude reduction as some of the signal energy is being transmitted into the second material. As there is a bond between the aluminum and the composite, some of the signal intensity may be refracted into the composite, and thus, there is a reduction in the return signal intensity that remains in the aluminum.

The reflection coefficient is a term that uses the acoustic impedances of the two materials to quantify the percentage of the ultrasound signal that reflects at a material interface given as (see e.g. [22])

$$R_{unbonded} = \frac{Z_{al} - Z_{air}}{Z_{air} + Z_{al}} \times 100\% \qquad (1)$$

$$R_{bonded} = \frac{Z_{al} - Z_{cf}}{Z_{cf} + Z_{al}} \times 100\% \qquad (2)$$

where $R_{unbonded}$ represents the reflection coefficient for the unbonded case, R_{bonded} represents the reflection coefficient for the bonded case, Z_{al} is the acoustic impedance for aluminum, Z_{air} is the acoustic impedance for air, and Z_{cf} is the acoustic impedance for the carbon fiber laminate. Notice the reflection coefficient for the unbonded case indicates that the full amount (100%) of the wave propagates back toward the ultrasound probe, whereas in the bonded case, only 54.7% of the wave reflects back toward the transducer while the rest of the wave transmits into the laminate. This difference in the reflection coefficients assists in quantitatively explaining why the signal decays more quickly for the bonded case than for the unbonded case. Similarly, the percentage of the wave that is refracted into the second material can also be computed using the acoustic impedances of the two materials.

The Fast Fourier Transform (FFT) plots shown in Figures 2(b) and 2(c) are generated using Matlab's built-in FFT function using the gated region indicated by the horizontal blue line in each of the A-scans. This gated region captures the second reflection at the aluminum-to-composite bondline for each of the two cases. Note from the figures the bonded case has a local maximum between 2 and 3 MHz. Both cases also have a local maximum energy frequency near 4.5 MHz, which is just less than the probe operating frequency of 5 MHz. The high frequency portion of the ultrasound signal attenuates less quickly in the bonded case than it does in the unbonded case. By comparing the two FFT plots to one another, an inspector could distinguish between the bonded and unbonded locations by looking at the difference in the high frequency content of the signal. When the high frequency content attenuates less quickly, the inspector has located a bonded location. If the high frequency content attenuates more quickly, the inspector has located an unbonded location.

The contact probe test was duplicated, but with the transducer placed against the composite side of the part as indicated in Figure 3(a). Similar signal intensity and FFT results were compiled from the composite side as was observed in Figure 2 for the aluminum side, and these results are presented in Figures 3(b) and 3(c) for the unbonded and bonded cases, respectively. As with the signal from the aluminum side, there is a noticeable decay in the ringing of the signal for the bonded component versus the unbonded component as indicated in Figures 3(b) and 3(c) by the

blue gated region. It is worth noting that the amount of signal decay is less striking relative to the aluminum side as the signal itself in the unbonded part is decaying. This decay is to be expected as noted by [5, 6] where they demonstrated there will be more signal decay in the composite structure versus a classical solid, such as aluminum. Regardless, the drop in signal intensity when sampling from the composite side of the part between the bonded and unbonded components is apparent in the figure. As observed in Figure 2, the FFT plot for the unbonded location indicates the high frequency content of the signal attenuates more quickly that at the bonded location. The unbonded location in Figure 3(b) has a peak energy frequency near 1.8 MHz whereas the bonded location in Figure 3(c) has a peak energy frequency near 2.5 MHz, which was also observed in FFT associated with the bonded location in Figure 2. The peak occurs at this lower frequency since the high frequency components of the signal attenuate faster in the viscoelastic composite. In the case of Figure 2, the wave propagated through the aluminum and then through the composite. In Figure 3, the ultrasound wave propagates through the composite first with the frequency components greater than 2.5 MHz attenuating rapidly and where 2.5 MHz is 50% of the operating frequency of the probe. In Figure 3(b), where the results depict the Fast Fourier Transform associated with an unbonded region, there is a single peak located near 1.8 MHz indicating some signal attenuation of the higher frequencies. Conversely, Figure 3(c) has two peaks. The first peak occurs near 2.5 MHz, as previously noted, and the second peak occurs near 5 MHz, which is indicative of the wave propagating through the aluminum where it tends to propagate at a higher frequency closer to that of the operating frequency of the probe as discussed in Figure 2.

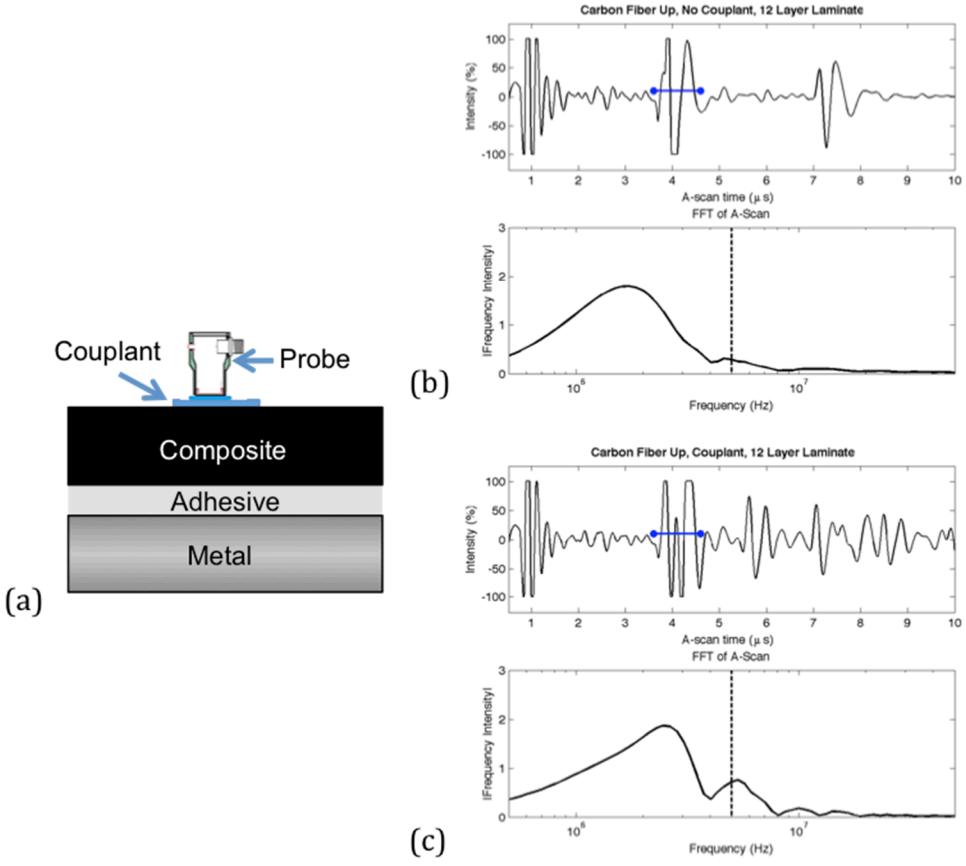

Fig. 3: Inspection of the bonded sample using a 5 MHz contact transducer. (a) The experimental configuration of the contact transducer measurements with the carbon fiber composite laminate in contact with the transducer. The A-scan results (top image) and FFT results (lower image) for, respectively, (b) an *unbonded* and (c) a *bonded* section of the interface. The dashed line in (b) and (c) refers to the transducer frequency.

As in the A-scan images provided in Figures 2(b) and 2(c), the blue gates in the A-scans observed in Figures 3(b) and 3(c) highlight the difference in signal amplitude between the unbonded case and the bonded case, respectively. Notice in Figures 3(b) and 3(c) that the decrease in A-scan signal amplitude is readily apparent and that the shape of the signal is considerably different between the two images. For example, look at the 5.5 μs location in the A-scans provided in Figure 3(b) and 3(c). Figure 3(c) has a peak located near 5.5 μs that is not observed for the unbonded location. This peak in Figure 3(c) indicates the backwall of the aluminum. Once the backwall of the aluminum has been detected, the ultrasound wave continues to echo between the front and back surfaces of the aluminum, which causes the structure of the A-scan to appear more complex due to the interference caused by the echoing wave as compared to that for the unbonded location.

4.0 – Bondline Detection using an Immersion Method

An immersion ultrasound technique was also used to inspect the bondline between the laminated 8 harness-satin layered composite and the aluminum steps depicted in Figure 1. The sample used for the analysis presented in this section was manufactured using the co-cure technique where the laminate is placed directly on the aluminum, and the bond between the two materials is formed during the laminate's cure cycle. The sample was inspected using a Mistras UPK-T36 ultrasound system with a 10 MHz spherically focused ultrasound probe operating in pulse-echo mode, and all data analysis was performed in-house using a custom MATLAB code to stitch the individual a-scans into the c-scans.

Using the co-cure method of fabrication, bonds between the carbon fiber lamina and the aluminum plate are formed as the resin begins to cross-link. These bonds are strong enough to hold the cured laminate to the aluminum plate for many applications. During the cure cycle, there are significant stresses induced into the part between lamina and the aluminum plate due to the mismatch of the coefficient of thermal expansion with the greatest stresses occurring at the corners of the part (see e.g., [23]). These high stresses will cause the thermoset bonds at the aluminum's surface to fail causing a delamination. Figures 4 and 5 show the C-scan immersion results obtained for the co-cured sample of the 12 ply system depicted in Figure 1. Figure 4 corresponds to the aluminum side facing the transducer while Figure 5 corresponds to the composite side facing the transducer.

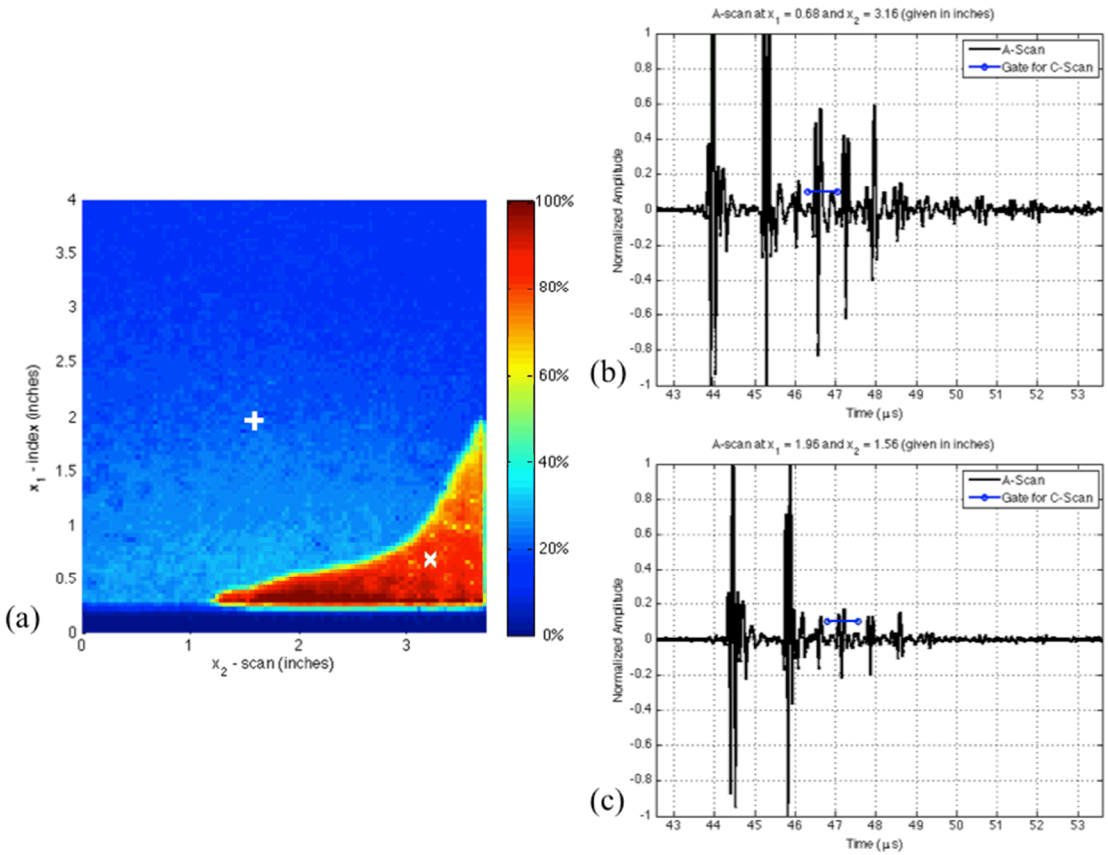

Fig. 4: (a) This image represents the C-scan obtained while inspecting the aluminum-to-composite bondline for the 12 ply laminate. The red region represents an unbonded location whereas the blue region represents a bonded region. (b) The A-scan signal associated with the unbonded location as marked by the 'x' in the C-scan. (c) The A-scan associated with the bonded location as marked by the '+' in the C-scan.

Figure 4(a) is the C-scan obtained from inspecting the co-cured sample with the aluminum side facing the transducer. The C-scan is obtained by gating the individual A-scans around the bondline within the part as indicated by the horizontal blue lines in Figures 4(b) and 4(c), with the color scale of the C-scan corresponding to the peak intensity within the gate. Figure 4(b) is the A-scan associated with the unbonded location marked by the 'x' in the C-scan, and Figure 4(c) is the A-scan associated with the bonded location marked by the '+' in the C-scan. When evaluating the C-scan image, the bonded area between the aluminum and the 12 ply composite is blue in color indicating a weak or non-existent signal whereas the unbonded area is red corresponding to increased signal intensity in the gate. This difference in color allows for quick identification of physical abnormalities (i.e. disbonds) between the two materials. The location of the disbond is as expected at the lower right edge of the part, which corresponds to one of the two corners of the 12-ply structure that is exposed to a free boundary condition and where the highest internal stress concentrations exist (see e.g., [23]).

Inspection of the A-scans associated with the two locations marked on the C-scan shown in Figures 4(b) and 4(c) indicates that the unbonded region has higher signal amplitude than the bonded region in the gated region. To emphasize this difference in signal amplitude, the second signal reflection from the bondline between the two materials in Figures 4(b) and 4(c) has been highlighted using the blue horizontal gates. The second reflection was chosen because the first

reflection signal saturated the receiver. The difference in the signal amplitude between the bonded and unbonded regions is caused by the acoustic impedance mismatch between the materials. When the ultrasound wave traveling through the aluminum plate encounters an unbonded region, the overwhelming majority of the wave reflects back toward the transducer due to the acoustic impedance of air. When the ultrasound wave traveling through the aluminum encounters a bonded location, a portion of the wave will continue to propagate into the composite material leaving a smaller fraction of the wave to reflect back through the thickness of the aluminum. Thus in regions where there is a disbond, a greater intensity of the signal should remain upon later reflections.

Figure 5 shows the C-scan results obtained when the co-cured part is turned over such that the carbon fiber reinforced laminated composite is facing the ultrasound transducer. The image in Figure 5(a) is the C-scan of the ultrasound scan data obtained from inspecting the 12 ply laminated composite-to-aluminum bondline with the gating for the A-scans selected to correspond to the depth where the bondline occurs. Figure 5(b) is the A-scan corresponding to the unbonded location, and Figure 5(c) is the A-scan associated with the bonded location as indicated in the C-scan.

When comparing the bonded location with the unbonded location in the C-scan in Figure 5, there remains a distinction in the color associated with the signal as in Figure 4. The bonded location is a royal blue color whereas the unbonded location is a bright turquoise color corresponding to higher signal intensity in the gated region of the A-scans. When inspecting the part, this difference in color provides a quick visual cue to a technician that there is something physically different between these two locations.

Figure 6 represents the C-scans obtained when inspecting the sample with the aluminum side facing the ultrasound probe and gating the aluminum-to-composite interface associated with each of the three laminate thicknesses. The leftmost portion of this figure corresponds to the 12 ply laminate section, the middle image corresponds to the 8 ply laminate section and the rightmost image corresponds to the 4 ply laminate section. The three portions of this figure were generated independently from one another to account for the different gate locations and are presented in the same figure for comparison purposes. In each of these three C-scans, the unbonded and bonded locations can be identified, with the majority of the unbonded locations occurring near the edges of the sample. The unbonded locations are associated with the increased signal intensity, which are primarily located along the edges of the sample where the highest residual stresses are located post-manufacturing. Figure 7 presents the image obtained from a single scan of the entire sample surface with the aluminum side facing the transducer. The gated region used for generating this image was located at the aluminum-to-composite interface for the 12 ply laminate region, and this gate is not the same as those associated with the other two regions. However, the regions of bonded and unbonded locations can still be identified for all three regions even though the gate is not capturing the actual bondline interface associated with the 8 and 4 ply laminate regions. This observation suggests that placing the gate at a single location may assist a technician or inspector by providing a more efficient method for inspecting a part with internal step discontinuities.

The same procedure as described in the previous paragraph was also applied to the data obtained from inspecting the sample with the composite side facing the transducer, and the results are presented in Figures 8 and 9. Figure 8 corresponds to the C-scans obtained for each of the three sections of the sample with the leftmost C-scan corresponding to the 12 ply laminate region, the middle C-scan corresponding to the 8 ply laminate region and the rightmost image corresponding to the 4 ply laminate region. The gates used in Figure 8 correspond to the composite-to-aluminum interface for each of the three regions, whereas the gate used in Figure 9 corresponds to the composite-to-aluminum interface in the 12 ply laminate region. From Figure 9, the unbonded region is clearly visible in the 12 ply laminate region; however, the distinction between bonded and unbonded regions appears more difficult in the 8 and 4 ply laminate regions when the same gate is used for generating the entire image. When inspecting the sample with the composite side, the most accurate identification of the bondline is presented when a separate gate is considered for each of the three laminate regions as seen in Figure 8.

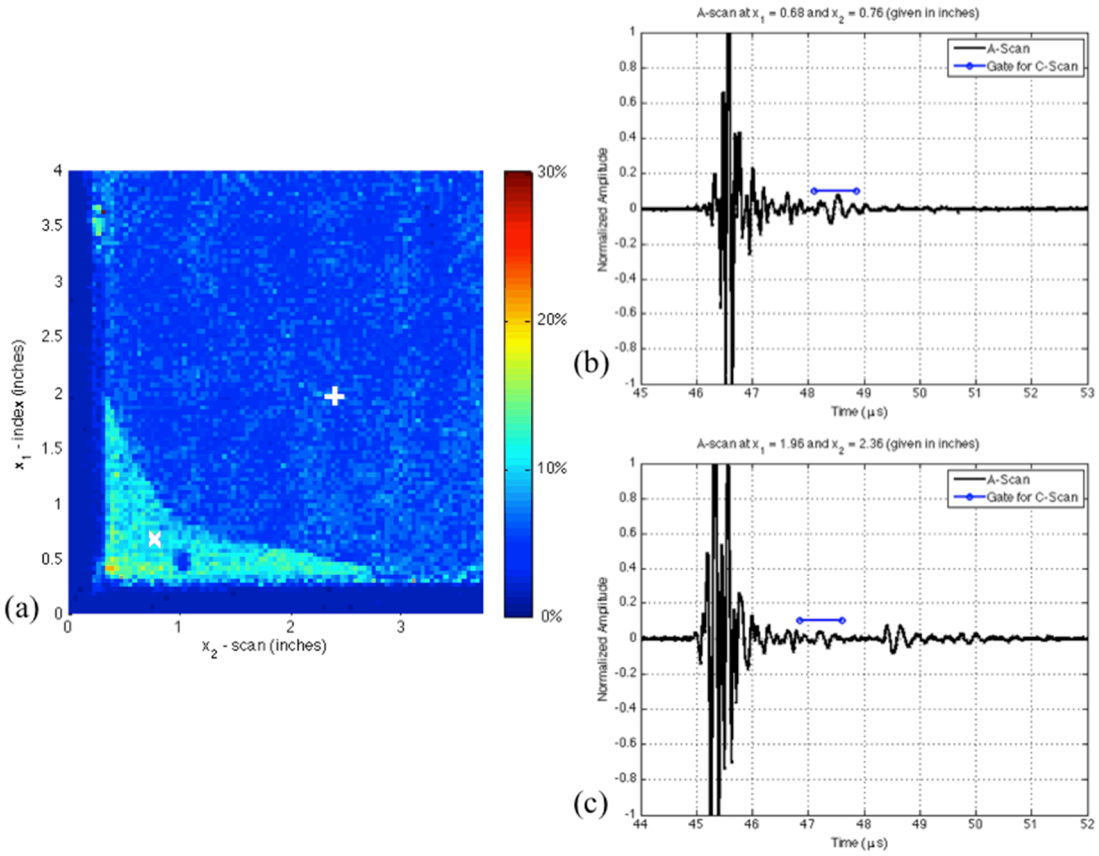

Fig. 5: (a) The C-scan obtained while inspecting the 12 ply composite-to-aluminum bondline. (b) The A-scan obtained at the unbonded location marked by the 'x' in the C-scan. (c) The A-scan obtained at the bonded location marked by the '+' in the C-scan.

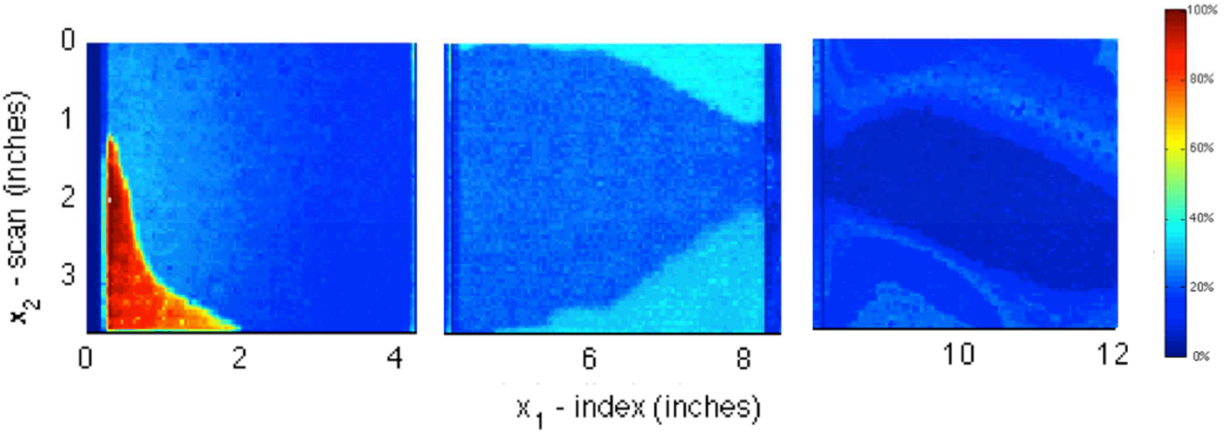

Fig. 6: The C-scan image results for the immersion ultrasound testing with the aluminum surface facing the transducer. The 12 ply laminate section is furthest left, the middle section corresponds to the 8 ply laminate, and the far right corresponds to the 4 ply laminate. Each of the three sections was plotted separately based on analyzing the gate associated with the interface for each of the laminate thicknesses. Thus, each plot represents a different plane of depth within the part.

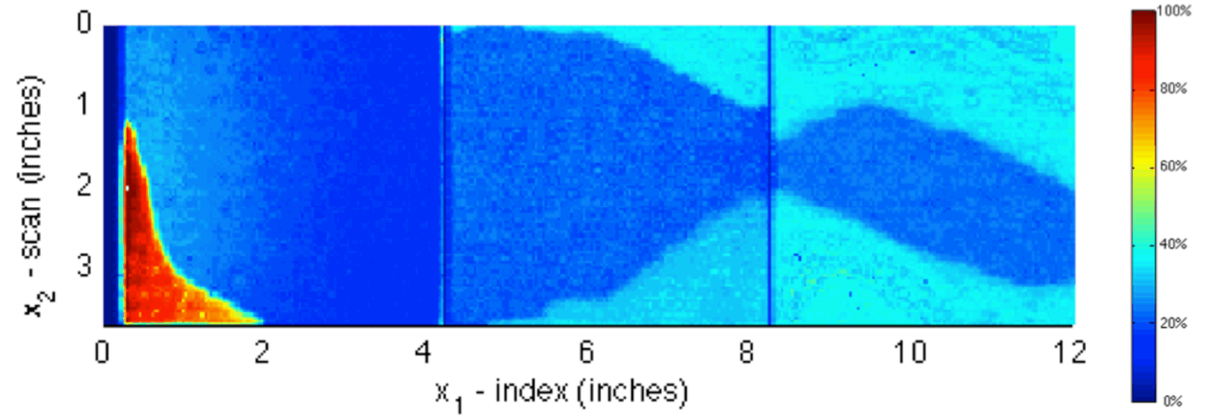

Fig. 7: The C-scan image results for the immersion ultrasound testing with the aluminum surface facing the transducer. The 12 ply laminate section is furthest left, the middle section corresponds to the 8 ply laminate, and the far right corresponds to the 4 ply laminate.

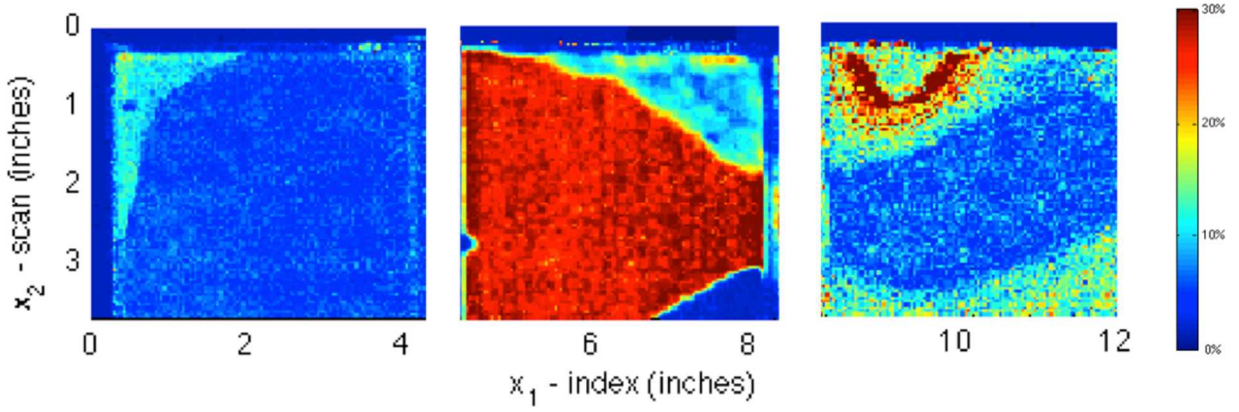

Fig. 8: The C-scan image results for the immersion ultrasound testing with the carbon fiber reinforced laminate surface facing the transducer. The 12 ply laminate section is furthest left, the middle section corresponds to the 8 ply laminate, and the far right corresponds to the 4 ply laminate. Each of the three sections was plotted separately based on analyzing the gate associated with the interface associated with each of the laminate thicknesses. Thus, each plot represents a different plane of depth within the part.

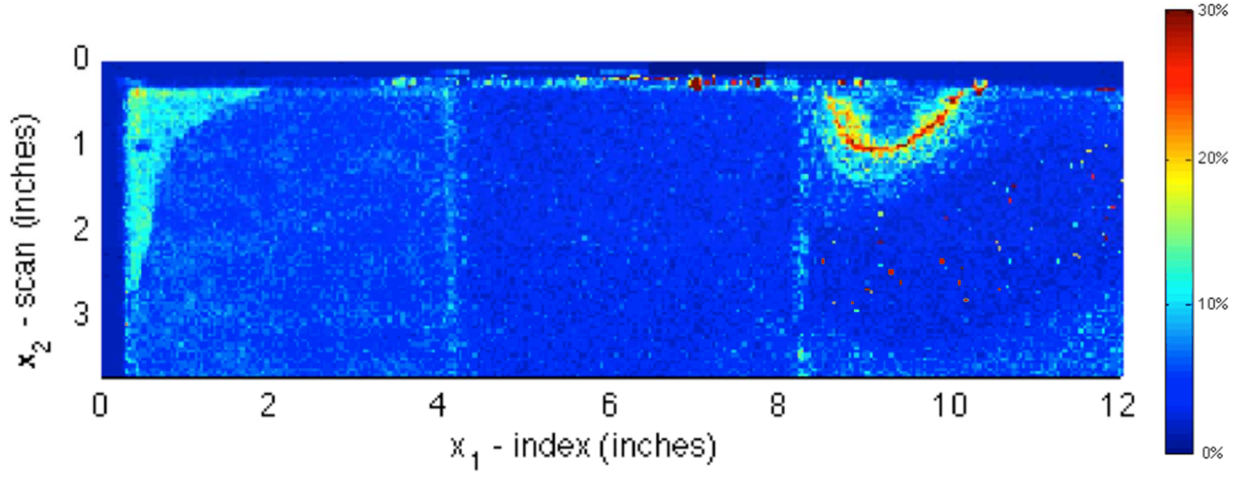

Fig. 9: The C-scan image results for the immersion ultrasound testing with the carbon fiber laminate surface facing the transducer. The 12 ply laminate section is furthest left, the middle section corresponds to the 8 ply laminate, and the far right corresponds to the 4 ply laminate

5.0 – Fast Fourier Transform Analysis of Immersion Results

The A-scans depicted in Figures 4 and 5 for the co-cured 12 ply laminated were further investigated using an in-house program constructed in MATLAB by capturing the frequency intensities using a Fast Fourier Transform. The frequency intensity plots were constructed by taking the Fast Fourier Transform of the data within the gated regions depicted in Figures 4 and 5. For each sample set investigated the gate is placed at the aluminum-to-composite bondline of the part, and the results of the co-cured part are presented in Figure 10 and Figure 11 for, respectively, the aluminum side facing the transducer and the composite side facing the transducer..

The frequency spectrum plot depicted in Figure 10 is taken from the aluminum side of the co-cured laminate with the gating shown in Figures 4(b) and 4(c). Notice that there is very little

change in the nature of the frequency spectrum when comparing the A-scan over the disbond (red line) versus the bonded (blue line) region of the laminate, corresponding to, respectively, the "x" and "+" marks in Figure 4(a). The difference comes in the relative intensity of the various frequencies. Secondly, notice that the frequency associated with the peak frequency intensity for both the bonded and unbonded locations remains nearly the same at approximately 7.5 MHz, which is lower than the operating frequency of the probe (10 MHz) given by the black vertical line in the figure. For signals obtained from the aluminum side of the sample the attenuation of frequencies appears to be independent of the presence of a disbond since the shape of the curve is similar for both the bonded and disbonded regions. The intensity of the frequency spectrum is a function of whether a bond or a disbond is present between the two materials as seen in Figure 10 where the two curves have significantly different intensities. Although the FFT plot does not provide new information regarding the identification of bonded versus unbonded locations at the interface between the two materials, it does provide information regarding the frequencies at which the wave tends to propagate through the thickness of the sample.

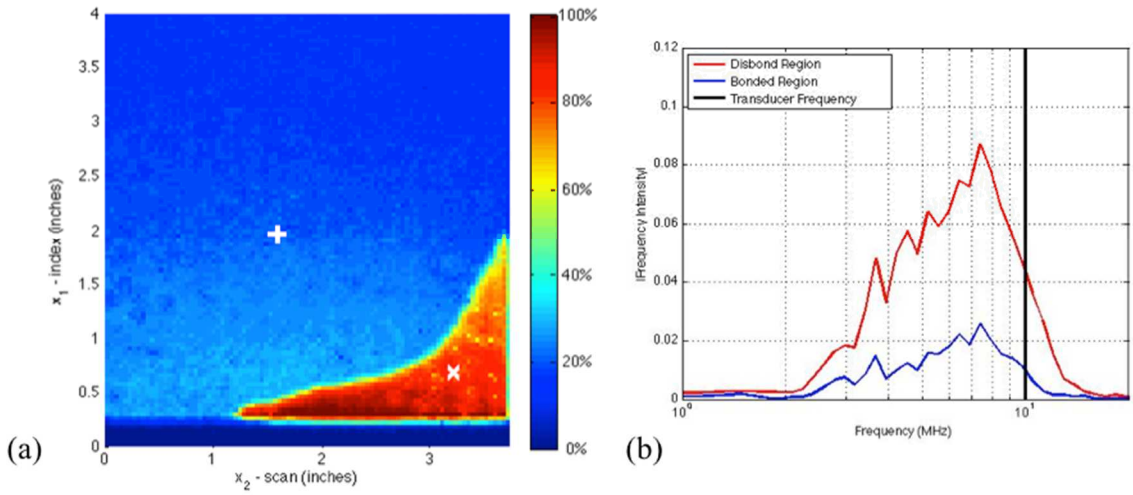

Fig. 10. (a) The C-scan of the aluminum-to-composite interface and (b) FFT of the ultrasound signal associated with the disbonded (red) and bonded (blue) locations indicated by the 'x' and '+', respectively, on the C-scan image in (a).

The frequency analysis is also performed on the signals from Figure 5(b) and 5(c) for scans obtained from the carbon fiber composite side of the co-cured part. The results of the frequency spectrum analysis are shown in Figure 11 with the same frequency intensity (vertical axis) scale shown in Figure 10 for samples taken from the aluminum side. The most obvious difference between the aluminum side and the composite side is the intensity of the signal, as much of it has diminished due to the attenuative nature of the resin. Looking just at the composite side scan, the frequency intensity for the unbonded location is significantly larger in amplitude than the frequency intensity of the bonded location where there is very little signal within the gate. Furthermore, both the bonded and unbonded locations exhibit a peak frequency near 3.5 MHz. It is interesting to note that the peak frequency of approximately 3.5 MHz from the composite side is lower than the peak frequency of the aluminum side, which was about 7.5 MHz. This decrease in the peak frequency is expected since the signal attenuation occurs at a faster rate for the higher frequencies propagating in a viscoelastic material, such as the composite laminate. Thus, there

will be a faster reduction of the peak frequency in the composite relative to the aluminum.

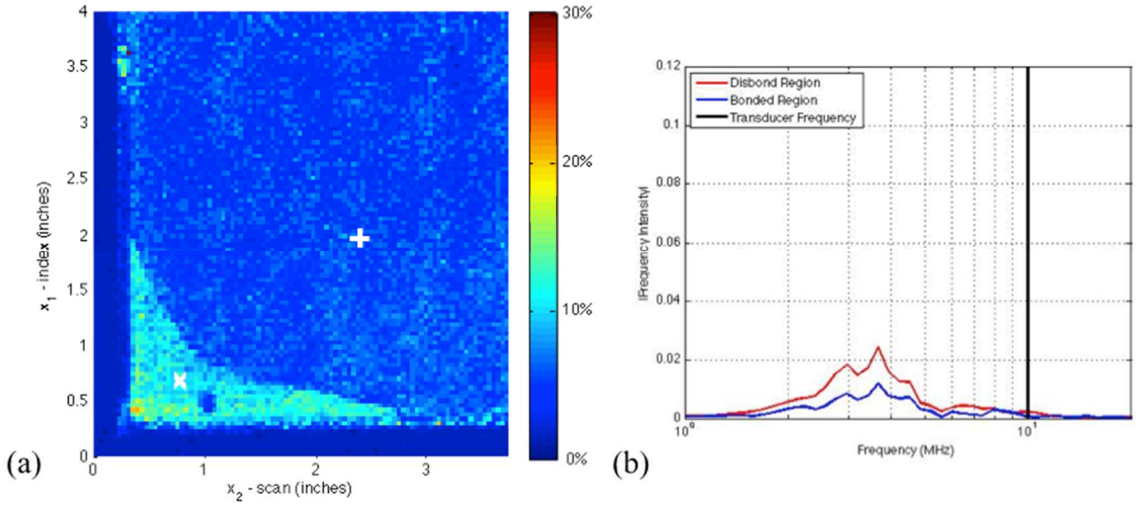

Fig. 11. (a) The C-scan for the composite-to-aluminum interface and (b) the FFT of the ultrasound signal associated with the disbonded (red) and bonded (blue) locations indicated by the 'x' and '+', respectively, on the C-scan image in (a).

6.0 – Conclusions

This paper investigates contact and immersion ultrasound methods for characterizing the bondline between a carbon fiber reinforced laminated composite and aluminum. The results demonstrated the presence or lack of an acoustic bond between the two materials, but do not provide a quantifiable metric as to the strength of the bond itself. Both the contact and the immersion pulse-echo ultrasound methods are able to detect whether or not a bond is present between the aluminum and the laminated composite, and these methods are able to make this identification by scanning either side of the sample.

The frequency spectrum plots associated with the immersion ultrasound data were analyzed, and distinctions between the frequency spectrum for the bonded and unbonded locations were observed. From this experiment, the authors observed the frequency spectrum of the bonded location had a consistently smaller frequency intensity than the unbonded location for the aluminum-to-composite bondline case as well as for the composite-to-aluminum bondline case. Although frequency spectrum analysis did not necessarily provide additional information about the identification of a bonded or unbonded region between the two materials, this analysis did provide information regarding the frequencies at which the wave tends to propagate through the material. The wave propagates at higher frequencies (near that of the probe) while propagating through the aluminum and propagates at lower frequencies (near 50% that of the probe frequency) through the composite.

Both investigated ultrasound techniques were able to detect the presence of unbonded regions at the interface between a composite laminate and aluminum regardless of which side, aluminum or composite, is inspected. This is essential as the acoustic mismatch of the two materials is quite significant, and the need exists for non-destructive methods of bondline inspection of composites on metallic structures. The results presented from this study provide a better understanding of the

behavior of bonded interfaces between laminated composites and metal with the use of ultrasonic inspection. Results obtained with these inspection methods could be used to ensure safety and reliability of designs and parts that are currently in-service.

Acknowledgements
Sandia is a multiprogram laboratory operated by Sandia Corporation, a Lockheed Martin Company, for the United States Department of Energy's National Nuclear Security Administration under Contract DE-AC04-94AL85000.

This material is based upon work supported by the National Science Foundation Graduate Research Fellowship under Grant No. DGE-1356113. Any opinion, findings, and conclusions or recommendations expressed in this material are those of the authors(s) and do not necessarily reflect the views of the National Science Foundation.

Bibliography
[1] Smith, R. A. Composite Defects and Their Detection. *Materials Science and Engineering*, **3**, pp. 103-143, 2009.
[2] Summerscales, J. Manufacturing Defects in Fibre Reinforced Plastics Composites. *Insight*, **36**(12), December 1994. pp. 936-942.
[3] Vine, K., P. Cawley, and A.J. Kinloch. Degradation Mechanisms in Adhesive Joints and the Implications for NDE. *Review of Progress in Quantitative Nondestructive Evaluation,* Ed. D.O. Thompson and D.E. Chimenti, **509**, pp. 1301-1308, 2000.
[4] Nieminen, A.O.K. and Koenig, J.L. Macroscopic and Modern Microscopic NDE Methods for Adhesive-Bonded Structures. *Int. Jn. of Adhesion and Adhesives,* **11**(1), pp. 5-10, 1991.
[5] Ting, T. C. T., The Effects of Dispersion and Dissipation on Wave Propagation in Viscoelastic Layered Composites, *Int. Jn. Solids Structures*, Pergamon Press Ltd., **16**, pp. 903-911, 1980.
[6] Ting, C. S. and Sachse, W., Measurements of Ultrasonic Dispersion by Phase Comparison of Continuous Harmonic Waves, *Journal of the Acoustical Society of America*, New York, NY, **64**, pp. 852, 1978.
[7] Nikitin, A. N., Vasin, R. N., Ivankina, T. I., Kruglov, A. A., Lokajicek, T., and Phan, L. T. N., Peculiarities of Quasi-Longitudinal Elastic Wave Propagation through the Interface between Isotropic and Anisotropic Media: Theoretical and Experimental Study, *Crystallography Reports*, **57**(4), pp. 560-568, 2012.
[8] Baker, A., Bonded Composite Repair of Metallic Aircraft Components – Overview of Australian Activities. AGARD-CP-550, pp. 1-14, 1995.
[9] Baker, A., Issues in the Certification of Bonded Composite Patch Repairs for Cracked Metallic Aircraft Structures. *Proceedings of the 20th Symposium of the International Committee on Aeronautical Fatigue (ICAF)*, Seattle, Washington, July 1999.
[10] Adams, R.D. and P. Cawley. Defect Types and Non-Destructive Testing Techniques for Composites and Bonded Joints. *Construction & Building Materials*, **3**(4), December 1989.
[11] Wang, W., Li, B., and Rokhlin, S. I., Ultrasonic Reflectivity Determination of Interfacial Properties in Adhesive Joints of Aluminum Alloys. *Review of Progress in Quantitative Nondestructive Evaluation*, **10B**, Ed. D. O. Thompson and D. E. Chimenti, Plenum Press, New York, pp. 1311-1318, 1991.

[12] Cawley, P. and M.J. Hodson. The NDT of Adhesive Joints using Ultrasonic Spectroscopy. *Review of Progress in Quantitative Nondestructive Evaluation*, **8B**, pp. 1377-1384, 1989.
[13] Drinkwater, B. and Cawley, P., Measurement of the Frequency Dependence of the Ultrasonic Reflection Coefficient from Thin Interface Layers and Partially Contacting Interfaces. *Ultrasonics*, **35**, pp. 479-488, 1997.
[14] Drinkwater, B. W., Dwyer-Joyce, R. S. and Cawley, P., A Study of the Interaction between Ultrasound and a Partially Contacting Solid-Solid Interface. *Proceedings: Mathematical, Physical and Engineering Sciences,* The Royal Society Publishing, **452**(1955), pp. 2613-2628, December 8, 1996. Obtained from http://www.jstor.org/stable/52862. Obtained on: June 15, 2015.
[15] Vine, K., Cawley, P., and Kinloch, A. J., Degradation Mechanisms in Adhesive Joints and the Implications for NDE. *AIP Conference Proceedings, Review of Progress in Quantitative Nondestructive Evaluation*, Ed. by D. O. Thompson and D. E. Chimenti, **509**, pp. 1301-1308, 2000.
[16] Pilarski, A. and Rose, J. L. Ultrasonic Oblique Incidence for Improved Sensitivity in Interface Weakness Determination. *NDT International*, **21**(4), pp. 241-246, 1988.
[17] Drinkwater, B. W., Dwyer-Joyce, R. S. and Robinson, A. M., The Use of Ultrasound to Investigate Rough Surface Contact Phenomena. *Review of Progress in Quantitative Nondestructive Evaluation*, **18**, Ed. by D. O. Thompson and D. E. Chimenti, Plenum Press, New York, pp. 1455-1462, 1999.
[18] Webster, M. N. and Sayles, R. S., A Numerical-Model for the Elastic Frictionless Contact of Real Rough Surfaces, *Journal of Tribology – Transactions of the ASME*, **108**, pp. 314-320, 1986.
[19] Vijaya Kumar, R. L., Bhat, M. R. and Murthy, C. R. L., Some Studies on Evaluation of Degradation in Composite Adhesive Joints Using Ultrasonic Techniques. *Ultrasonics*, **53**, pp. 1150-1162, March 2013.
[20] Stair, S. L., Moore, D. G. and Nelson, C. L. Bondline Boundary Assessment of Cohesive Bonded Solid Woven Carbon Fiber Composites Using Advanced Diagnostic Methods. 19th World Conference on Non-Destructive Testing, Munich, Germany, June 2016.
[21] Stair, S. L., Jack, D. A., Moore, D. G., and Nelson, C. L., Investigation and Identification of the Bondline Between a Carbon Fiber Reinforced Laminated Composite and a Metal Structure via Ultrasonic Techniques, *Proceedings of Society of Plastics Engineers Automotive Composites Conference and Exhibition (ACCE)*, Novi, MI, September 2016.
[22] Schmerr, Jr., L. W. *Fundamentals of Ultrasonic Nondestructive Evaluation: A Modeling Approach*, Plenum Press, NY, 1998, pp. 93.
[23] Stair, S. and Jack, D.A., "Comparison of experimental and modeling results for cure induced curvature of a carbon fiber laminate," *Polymer Composites*, December 11, 2015, Obtained from http://onlinelibrary.wiley.com/doi/10.1002/pc.23838/abstract.